ECE 445

SENIOR DESIGN LABORATORY

FINAL REPORT

Wireless Fast Charging Autonomous Car

Team # 18

ZIYUE GUO (ziyueg3)
ZONGYANG ZHU (zz85)
YIZHI LI (yizhili2)
YIQUAN JIN (yiquanj2)

SUPERVISOR: CHUSHAN LI
TA: YU DOU

May 10, 2024

Abstract

In light of national carbon peaking and carbon neutrality goals, along with the rapid development of artificial intelligence, smart electric vehicles have become a crucial force driving the sustainable evolution of transportation. And also, wireless power transfer has been recognized as one of the top ten emerging technologies of the 21st century. Compared to conventional cable-connected power methods, wireless charging offers benefits in safety, convenience, cost saving and so on.

Our objective is to develop a vehicle that seamlessly integrates wireless charging, autonomous navigation, and obstacle avoidance functionalities. To achieve our goals, we have designed several PCBs to implement wireless charging functionality. As for the sensors, we utilized a combination of LiDAR and cameras for map construction and object recognition and tracking. Additionally, we have designed and installed a shock absorption chassis structure to enable the vehicle to adapt to complex driving environments.

Keywords: Smart Electric Vehicles, Wireless Charging, Autonomous Navigation, Object Tracking

Contents

1 Introduction

1.1 Problem

Current automobiles are not completely automatic since they cannot go charging automatically when uses up electricity. Another problem is the current charger occupies location so it may cause a waste of space. Our objective is to develop a vehicle that seamlessly integrates automatic wireless charging, autonomous navigation, and obstacle avoidance functionalities, enabling it to navigate its environment effortlessly while ensuring efficient energy replenishment.
Wireless charging cars may face several challenges. Efficiency loss due to electromagnetic interference and distance between coils is common, leading to slower charging and energy wastage. Precise alignment of charging coils is crucial, as misalignment affects charging efficiency. Interference from electronic devices and obstacles can disrupt charging. Heat generation during charging sessions poses risks to battery health.

1.2 Solution

A proposal is put forth for the development of an autonomous vehicle equipped with wireless fast charging capability. This vehicle is designed to autonomously detect the location of wireless charging stations and navigate to them swiftly and efficiently. In addition, the proposed autonomous vehicle will incorporate computer vision technology to enable obstacle avoidance, further enhancing its navigational capabilities. To save the space, the charging system is set at the ground of the vehicle instead of standing at the side of the vehicle.

1.3 External System

We require a ground-based charging station and a detailed map to facilitate the navigation of the vehicle. Additionally, we necessitate a personal computer to establish communication with the vehicle, enabling the issuance of diverse commands. The charging station comprises a DC voltage supply, a function generator, and a primary-side charging coil. A distinct red indicator will be positioned at the charging point for seamless localization by the vehicle. Utilizing cardboard material, we will fabricate the driving map, encompassing straightaways and various curvature configurations. Upon destination selection, the vehicle will autonomously traverse the map.

2 Design

2.1 Block Diagram

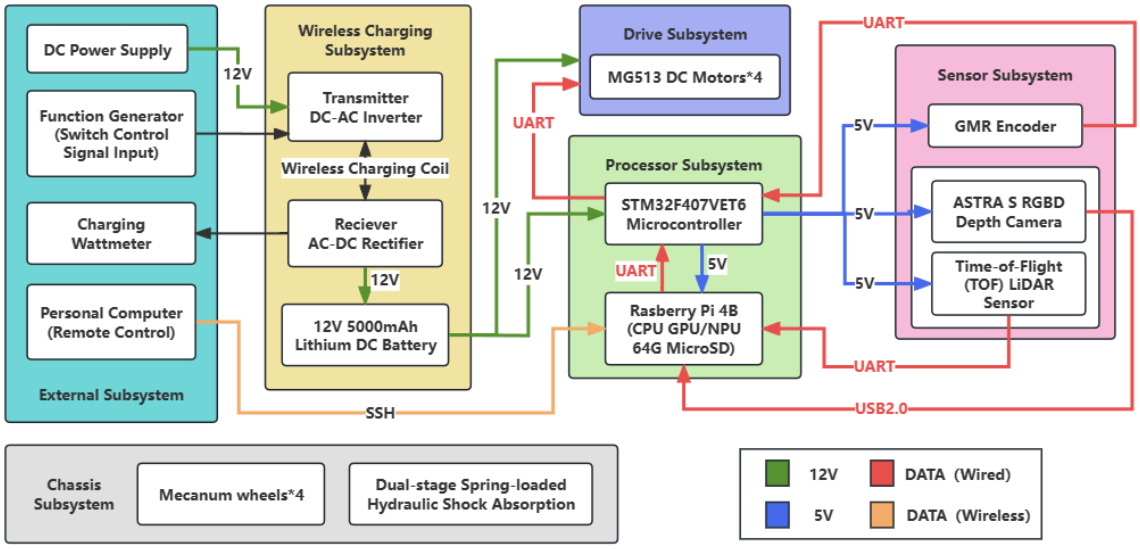

Figure 1: **Block Diagram**

2.2 Design Details

2.2.1 Physical Diagram

Figure 2 below is the latest CAD model of the cart. The main body part of the cart consists of four McNamee wheels, shock absorbing chassis and identification of detection components such as radars and cameras.

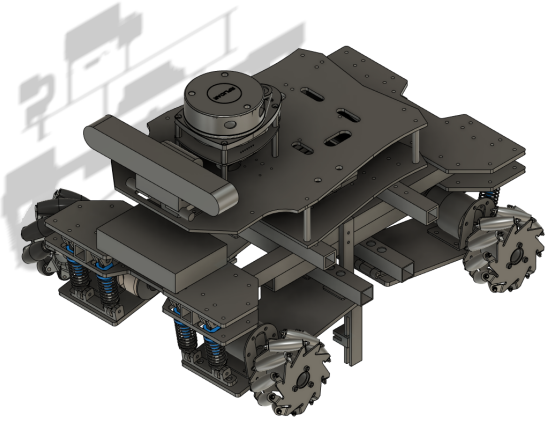

Figure 2: **Physical Diagram**

2.2.2 Wireless Charging Subsystem

Overall, we have chosen to utilize the inductive power transfer (IPT) system, which can transfer power from the primary coil of the loosely coupled coils to the secondary coil, with transmission distances typically ranging from millimeters to centimeters and characterized by high-efficiency transmission.

In details, the wireless charging subsystem comprises two main components: the transmitter and the receiver. At the transmitter end, a direct voltage power source is connected to a high-frequency inverter to convert the DC power into 85kHz AC power suitable for wireless charging. When powered, an alternating electromagnetic field is generated near the primary coil. The receiver, installed on the electric vehicle, includes a secondary coil to capture energy from the oscillating magnetic field. The receiver primarily consists of a rectifier, with its output connected to the vehicle's DC battery. When the vehicle is parked over the base station, it receives the oscillating magnetic field, inducing a current in the vehicle's secondary coil.

Additionally, we employ series-series (S-S) compensation to achieving constant voltage output by connecting compensation capacitors in series with the circuits. In the IPT system, the compensation network is essential for resonating with the self-inductance of the primary and secondary coils to produce sufficient magnetic fields for energy transmission. Moreover, the compensation network can compensate for reactive power, significantly reducing component stress and facilitating the realization of high-efficiency wireless charging systems.

It is worth noting that we must ensure the safety of the charging process to prevent dangers such as overcharging of the battery or circuit short circuits. Therefore, we have designed voltage and current sampling functions and utilized the ADC function of the STM32 micro-controller to convert them into digital signals. When the charging voltage exceeds the full charge voltage of the lithium battery, the buzzer will sound to indicate full charge. We have also added a power meter on the vehicle to display real-time charging power and other parameters.

2.2.3 Drive Subsystem

The drive subsystem of the intelligent car responds rapidly to instructions provided by the processor system and ensures smooth and accurate control over the car's movement in various directions, including forward, backward, left, right, and even turning in place. The drive subsystem primarily consists of the MG513 metal gear reduction motor, clamping type couplers, motor brackets, and other components. The four motors are mechanically connected to the four Mecanum wheels and mounted on the chassis subsystem, powered by the power subsystem, and controlled by the processor subsystem. Specifically, the car requires four DC reduction motors, consisting of full-metal gear reduction boxes and GMR encoders from the sensor subsystem. The selected motors have a rated voltage of 12V, a rated current of 0.36A, a reduction ratio of 30, and a power of approximately 4W. The rated torque of the motors is 1kg.cm, and the unloaded speed after reduction is 366±26rpm. We estimate that the motors can drive the car at a maximum speed of

approximately 1.2m/s and can carry a maximum weight of 3-4kg, which fully meets our requirements.

2.2.4 Sensor Subsystem

LiDAR Sensor We used Leishen N10P radar sensor to implement 2D obstacle avoidance functionality, which is a commercial-grade Time-of-Flight (TOF) LiDAR sensor, with a measurement range of 25 meters, a sampling frequency of 5400Hz, and a serial interface for communication. This radar implemented the function of detecting obstacles on both sides and in front of the vehicle, including roadblocks and walls, allowing for timely adjustments to the vehicle's trajectory as necessary. By making the car move within a certain range, a relatively complete 2D map can be established. The continuous red dots in the construction process are the obstacles detected by the radar in real time, while the black dots are the obstacle boundaries determined by the radar.

After the drawing is completed, the car can begin to navigate. During the navigation process, when the planned path meets a relatively narrow point, the car may stop because it is judged that it cannot pass, but the actual car can fully pass the gap between obstacles, because we set the expansion radius for the obstacles, and within the expansion radius, it is still considered that the obstacles cannot pass, which can be solved by modifying the expansion radius.

RGB Depth Camera The ASTRA S RGBD camera features a depth range of 0.4 to 2.0 meters, with a power consumption of less than 2W and a peak current of under 500mA. Its depth field of view spans horizontally at 58.4 degrees and vertically at 45.5 degrees, while the color field of view extends horizontally at 63.1 degrees and vertically at 49.4 degrees. Data transmission is facilitated via USB 2.0 connectivity.

In the design, we used this camera for visual tracking function, and we designed several common colors in advance to provide recognition, including red, blue, yellow, and green, which are determined by the HSV range. After turning on the visual tracking function, the camera will detect color blocks and distance information within the front sector area, and hand it over to the main control to calculate its contour line and approach route. Then the car will drive towards the object of that color and maintain a certain distance, such as 30cm, continuously.

2.2.5 Processor Subsystem

Raspberry Pi 4B Our ROS (Robot Operating System) controller is based on the Raspberry Pi 4B, featuring a quad-core ARM Cortex-A72 processor clocked at 1.5GHz, 4GB of RAM, with a computational power of 0.2 TOPS. It operates on a 5V power supply. The ROS controller, running on the Raspberry Pi 4B, establishes connections and controls the camera and LiDAR sensor via their respective interfaces. The camera, operating through a USB 2.0 connection and supporting the UVC standard, streams RGB images to the Raspberry Pi. These images are processed using ROS-compliant computer vision algorithms.

STM32 microcontroller Furthermore, we use the STM32 microcontroller to provide supply voltage to the Raspberry Pi 4B and the sensor subsystem and receive data from them. The STM32 microcontroller can also provide control signal to the drive subsystem. STM32 Controller Integrated Dual 5V Power Supplies: The STM32 controller is equipped with two 5V power outputs. One 5V power supply powers the STM32 controller and peripherals (such as encoders, Bluetooth, gamepads, etc.), while the other 5V power supply is used to power the Raspberry Pi.

2.2.6 Chassis Subsystem

In the shock subsystem, our design is mainly built around four independent hydraulic spring shock absorbers, and each wheel has its own independent shock absorption system, which can effectively ensures the leveling of the entire cart chassis and thus increase the efficiency of wireless charging. First of all we mounted four flat plates cut from acrylic sheets on the metal frame for linking the hydraulic spring shock absorbers to the metal frame and limiting the working space of the shock absorbers. The motor is mounted on a base plate made of aluminum alloy, which is connected to the bottom of the metal frame by means of hinges. The lower end of the shock absorber is also connected to the aluminum base plate by means of a linkage. (Fig.3)

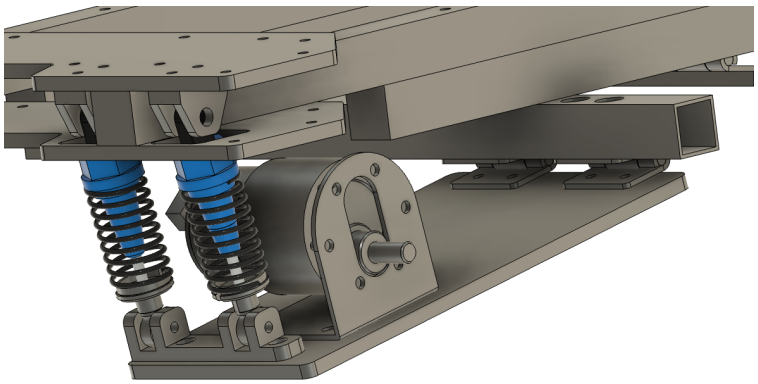

Figure 3: **Shock Absorption System**

In our design, the hydraulic spring shock absorber is mounted between the acrylic cut plate and the aluminum base plate (Fig. 4). When one of the wheels of the cart travels on the raised ground, the shock absorber located between the acrylic cut plate and the aluminum base plate is squeezed by the terrain and the gravity of the cart itself to maintain the balance of the cart's chassis. The hydraulic spring shock absorbers have a certain damping effect, when the terrain has a large undulation, the hydraulic spring shock absorbers can better alleviate the sudden change of the level state of the cart. The shock absorbs the repeated bouncing that occurs after various impacts from the road surface to accelerate the attenuation of the spring's inherent vibration, providing the cart with better driving smoothness. In addition to this, the shock absorber can also mitigate the

impacts of the road surface, quickly absorbing the vibrations generated during bumps and returning the cart to its normal driving condition.

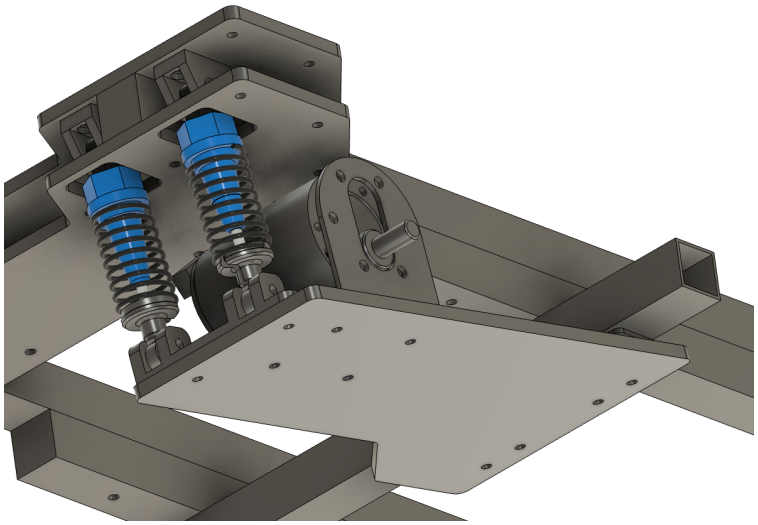

Figure 4: **Hydraulic Spring Shock Absorber**

2.3 Design Procedure

2.3.1 Wireless Charging Subsystem

Schematic Simulation Design We first utilize MATLAB Simulink to simulate the circuit of the wireless charging section to ensure the theoretical feasibility of the circuit. Our simulation circuit mainly consists of a high-frequency inverter and rectifier. It is worth noting that we use the equivalent circuit of same-side parallel connection of coupled inductors to replace the loosely coupled coils.

Wireless Coil Design For the design of the wireless coil, we initially designed a circular coil with a radius of 7.5 centimeters based on the size of the car chassis. All other conditions being equal, generally speaking, the larger the size of the wireless charging coil, the higher the charging efficiency. This is because larger coils can better capture the electromagnetic field generated by the transmitter and convert it into electrical energy. Larger coils can also accommodate more coil turns, increasing the induced voltage and current, further enhancing charging efficiency. However, excessively large coil sizes may increase costs, resistance, and may lead to additional heat dissipation issues. Nevertheless, we estimate that these factors have minimal impact on the overall circuit, and the charging system exhibits excellent heat dissipation.

To meet the project's requirements, we use multi-strand enamel-insulated wire for the excitation coil with a sufficiently large cross-sectional area. Multi-strand enamel-insulated wire for excitation coils typically refers to a type of conductor used in exciting electromagnetic devices. It consists of multiple strands of insulated wire or bare copper wire, often

coated or wrapped in insulating material to enhance electrical insulation performance. The main feature of this wire is its large surface area, which disperses alternating current, thereby mitigating the skin effect.

PCB Design The PCB for our project mainly includes the resonant circuit, inverter and MOSFET driver circuit on the transmitter side, and the rectifier resonant circuit and voltage and current sampling circuit on the receiver side. The completed portion of the PCB circuit, along with its schematic and layout, are shown in the appendix.

It's worth noting that we stabilize the DC voltage by parallel connecting a series of capacitors. In the circuit with parallel connected capacitors, when the voltage fluctuates, the capacitors absorb or release charges to maintain voltage stability. As the input voltage rises, the capacitors absorb charges and store energy. Conversely, when the input voltage drops, the capacitors release the stored energy, keeping the output voltage stable.

2.3.2 Sensor Subsystem

LiDAR Design We have designed an automatic driving car LiDAR system suitable for simulated urban roads. The requirements include real-time high-precision map construction, obstacle detection and tracking, traffic and charging identification, etc. Therefore, the LiDAR needs to have the capability of long-distance measurement and high resolution to ensure high-precision perception of the surrounding environment. Due to the directionality and monochromatic nature of laser, LiDAR has strong anti-interference ability to environmental disturbances and clutter signals, providing clear target signals. Additionally, obstacles in the simulated roads are very small in size, and LiDAR can provide distance measurements at the centimeter level, giving it an advantage in applications requiring fine target identification and environmental perception. We employ multiple algorithms to achieve functions such as point cloud filtering, obstacle detection and tracking, and map construction, ultimately ensuring the normal operation of the entire LiDAR system.

RGB Depth Camera The ASTRA S RGBD camera is a type of camera used to capture RGB (color) and depth information simultaneously. This camera can capture both color images and depth information for each pixel, typically achieved using infrared or other depth sensing technology. By combining RGB and depth information, it enables more accurate object detection, tracking, pose estimation, and other tasks, while also aiding in the creation of more realistic virtual environments or augmented reality applications.

2.3.3 Chassis Subsystem

In the process of designing the whole chassis system, we first modeled the metal frame and individual parts using software such as Solidworks and Autodesk Fusion, and we did the overall assembly on the software. After confirming that the dimensions and design made sense, we laser cut the aluminum square tubing, the aluminum plate and the acrylic plate, and we printed some of the tiny connectors through a 3D printer. After that we

chose the right oil pressure spring shocks to purchase. When all the parts were ready, we assembled them and assembled them with the motor, depth camera and radar to finalize the design and manufacture of the entire chassis section.

2.4 Design Alternatives

2.4.1 Wireless Charging Subsystem

We initially planned to use supercapacitors to power the vehicle because they provide rapid charging and discharging capabilities, with precise control over the magnitude of current flow. This allows for quick energy storage and release during short charging sessions while ensuring efficient energy management. However, compared to lithium batteries, supercapacitors have lower energy density. This means they require larger volume to store the same amount of energy, which our vehicle cannot accommodate. Additionally, supercapacitors have relatively high self-discharge rates, meaning they lose stored energy over a short period. For safety reasons, we opted for lithium batteries, which come with short circuit, overcurrent, overcharge, and overdischarge protection, and support charging while discharging.

2.4.2 Chassis Subsystem

The chassis subsystem consists mainly of a shock absorption system and a metal frame. In the shock absorption system, we initially planned to design the front wheels of the cart with a pendulum suspension system to act as a shock absorber (Fig.5). However, after testing and thinking, we found that the pendulum suspension system on the front wheels could not ensure the levelness of the chassis of our cart when facing some complicated and uneven ground, which might affect the efficiency of wireless charging, and finally we chose the independent shock absorber system composed of four independent hydraulic shock absorbers to keep the level of the cart.

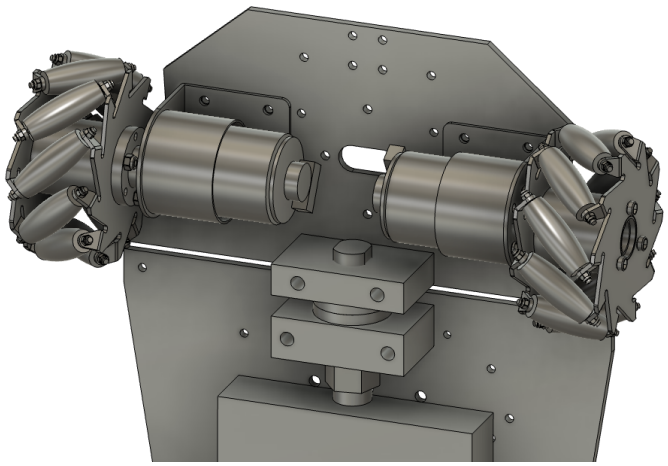

Figure 5: **Initial Shock Absorption System**

We also plan to install a metal plate on the initial chassis to protect the PCB and electronic components from magnetic fields during wireless charging. However, in the subsequent design we eliminated this part and utilized the metal frame in the chassis system and the metal plate in the shock absorption subsystem for the magnetic isolation protection.

3 Verification

3.1 Wireless Charging Subsystem

As for the verification of the wireless charging part, we utilized impedance analyzers, function generators, and other experimental devices to test the parameters of circuit components and simulate the equivalent circuits. Next, we use an electronic load to simulate the lithium battery for functional testing. Finally, the PCBs are installed on the car and connected with other subsystems to test the charging functionality. The specific verification steps are as follows:

Step one: Use an impedance analyzer to measure the impedance of the multi-strand enamel-insulated wire excitation coil wireless charging coil at different frequencies of AC current and store the results. Below are the impedance magnitude and phase angle curves I plotted on the impedance analyzer.

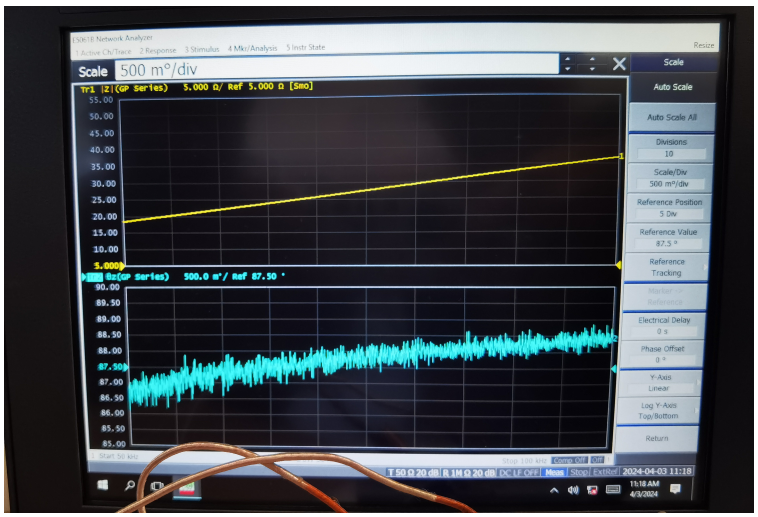

Figure 6: **Impedance Magnitude and Phase Angle Curves of the Coils**

Step Two: Since the frequency of the wireless charging's alternating current is 85kHz, I read the relevant values from the curve. To calculate the inductance L and the resonant capacitance C based on the impedance magnitude Z and phase angle θ of an AC circuit with frequency f, the formulas and results are as follows:

$$L = \frac{Z}{2\pi f \cos(\theta)} \tag{1}$$

$$C = \frac{1}{(2\pi f)^2 \cdot L} \tag{2}$$

Frequency (Hz)	Z (Ω)	Theta (degrees)	R (Ω)
84990.61914	31.86473485	88.13949206	1.034570882

Table 1: **Frequency, Impedance, Phase Angle, and Resistance**

X (Ω)	L (H)	C (F)
31.84793541	5.96391E-05	5.87988E-08

Table 2: **Reactance, Inductance, and Capacitance at Resonance**

Step Three: The two wireless coils can be equivalent to a weakly coupled transformer, and their equivalent can be converted into a same-side parallel connection of coupled inductors[1], and the power transmission of the circuit can be verified in MATLAB.

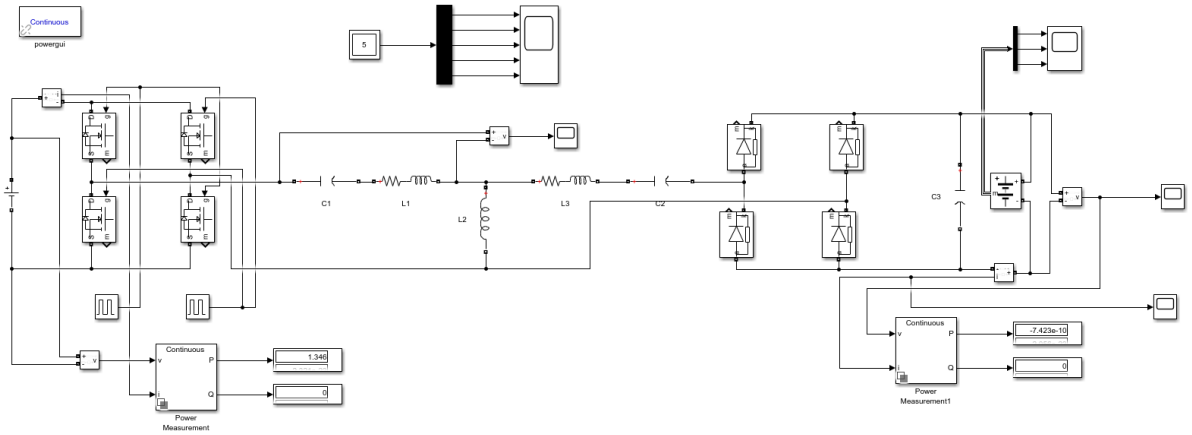

Figure 7: **Equivalent Circuit of Coupled Inductors in Parallel on the Same Side.**

Step Four: After soldering the components on the PCB, we connected the PCB to the fabricated coils. At this stage, we chose to use an electronic load instead of a lithium battery for testing the charging functionality. We set the electronic load to a constant voltage source of 12V, while monitoring the charging current and voltage. We then connected the transmitter side to the DC supply and the function generator, providing 15V for the MOSFET drive voltage and 12-36V for the input voltage. The function generator outputs two complementary 85kHz square waves as the control signals for the MOSFETs.

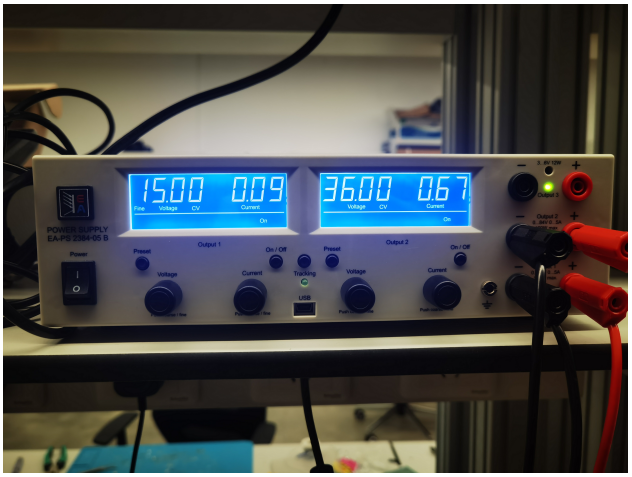

Figure 8: **The DC supply input during the verification process.**

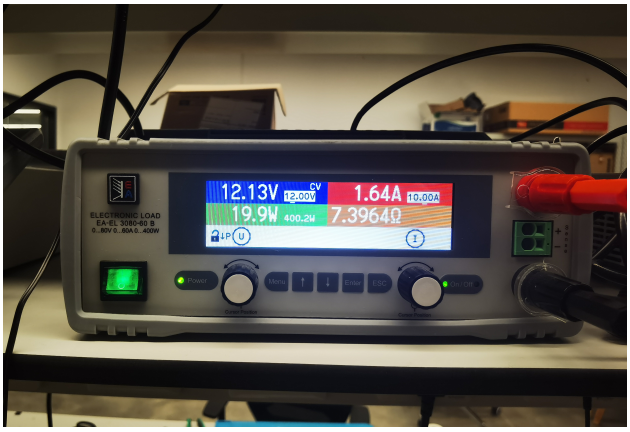

Figure 9: **The output of electronic load during the verification process.**

Additionally, we used an oscilloscope to measure parameters such as the voltage across the compensation capacitors, the voltage across the coils, and the current within the coils on the transmitter side circuit. (Fig. 10)

- Channel 1 captures the switching signal of the transmitter inverter.
- Channel 2 measures the voltage across the coil.
- Channel 3 records the AC voltage output from the inverter.
- Channel 4 measures the current flowing through the coil.

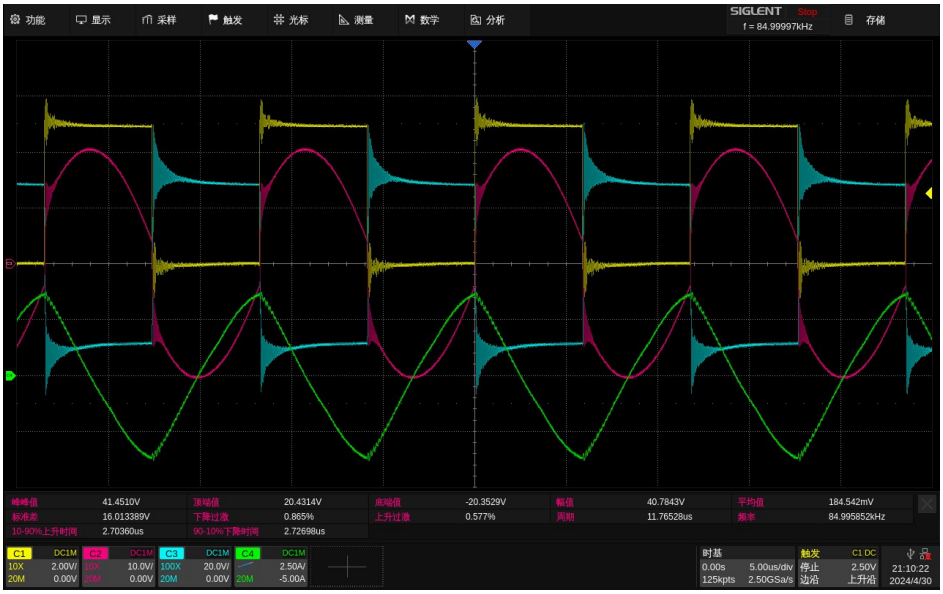

Figure 10: **The Oscilloscope Display During the Verification Process.**

Initially, we chose to position the primary and secondary coils as close as possible to minimize the effects of mutual inductance. When the input voltage was set to 36V(Fig.8), we observed that the electronic load displayed a wireless charging power of 19.9W(Fig.9).

Step Five: To optimize the charging efficiency of our wireless power transfer system, we adjusted the distance between the two coils to vary the mutual inductance, aiming to bring the circuit closer to resonance while keeping other parameters constant. After extensive testing, we determined that a distance of 3cm was optimal. This distance was then fixed using a mechanical support structure on the vehicle chassis.

Step Six: Subsequently, we connected a power meter to the circuit to measure the charging voltage, current, and power. The STM32 micro-controller was used to supply 5V power to the power meter. Finally, we placed the vehicle over the charging point to conduct a comprehensive test of our wireless charging functionality.

	Voltage(V)	Current(A)	Power(W)
Input	21.0	1.1	23.1
Output	15.93	1.316	20.97

Table 3: **Wireless Charging Input and Output Values**

We measured the input power and output power of the wireless charging system.4.1 We found that the power loss between the two is minimal, which demonstrates that our wireless charging system is relatively well-designed and successful.

3.2 Sensor Subsystem

LiDAR Subsystem After starting the SLAM mapping process, the LiDAR would start detecting the surrounding environment. As the figure shows, the black line represents the boundary and the blank part means the vehicle could safely go through. After going through all the paths, the cost map is established. Then the vehicle could automatically get to the specified destination by using the g-mapping algorithm to find the best path (Fig. 11).

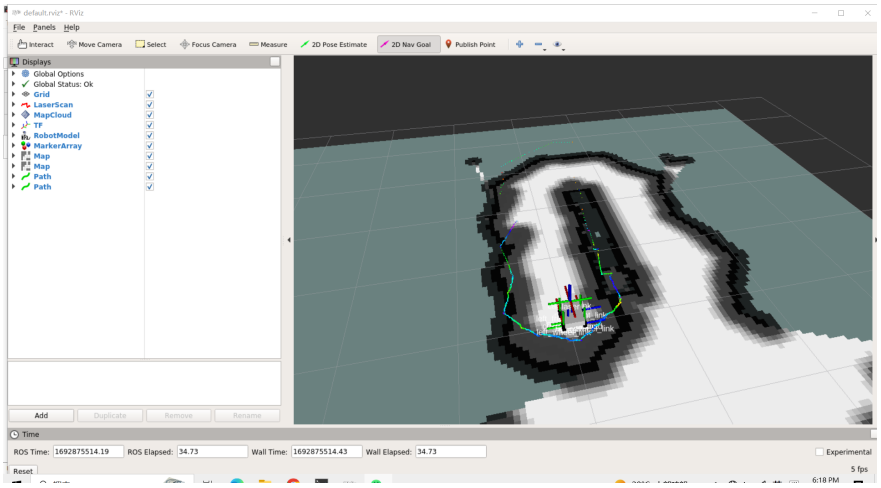

Figure 11: **SLAM Mapping.**

RGB Depth Camera For the block with the selected color (we use red in this situation) in the field of view, the camera will combine RGB information and depth information to extract the color block. Then, after blurring and convolution kernels, we can calculate the contour line of the color block, so that the car can approach the color block in that direction. Finally, the color block will remain in the center of the car's field of view (Fig. 12).

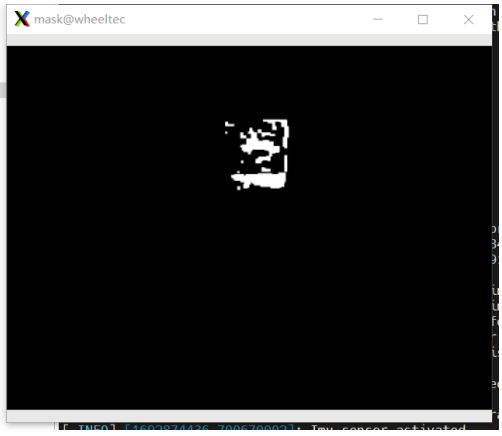

Figure 12: **Recognition of the contour lines of the color block.**

3.3 Chassis Subsystem

Figure 13 and Figure 14 show the stress distribution and the deformation displacement of right angle connectors respectively. Figure 15 and Figure 16 show the stress distribution and the deformation displacement of flanged metal connectors. In our design, the materials of the connectors are all carbon steel, which has high hardness and strength. According to Figure 14 and Figure 16, we can see that the maximum displacement of the right-angle connector under stress is 0.129mm and the maximum displacement of the flanged metal connection under stress is 5.396E-05mm, which all meet the design requirements. In our real-world tests, these connectors can effectively support the weight of the cart.

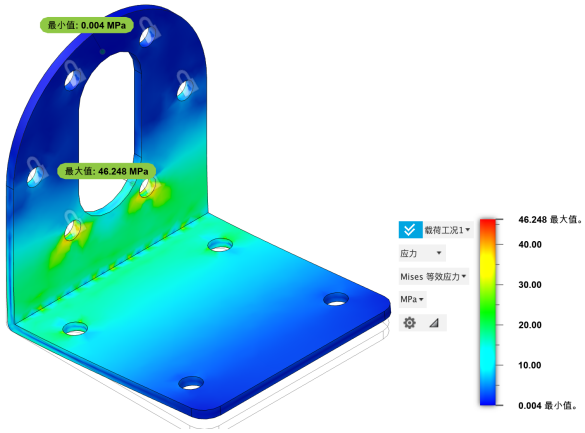

Figure 13: **Right-Angle Connectors Stress**

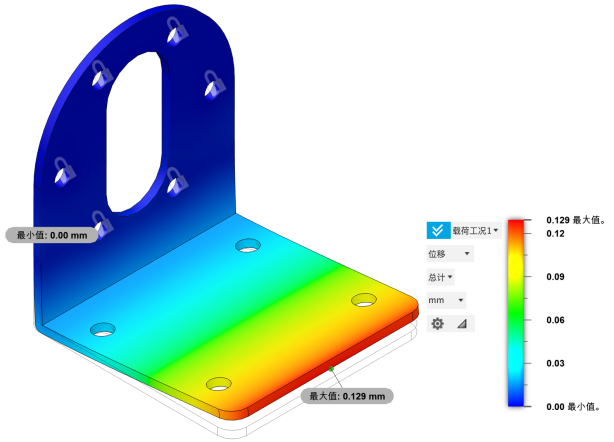

Figure 14: **Right-Angle Connectors Displacement**

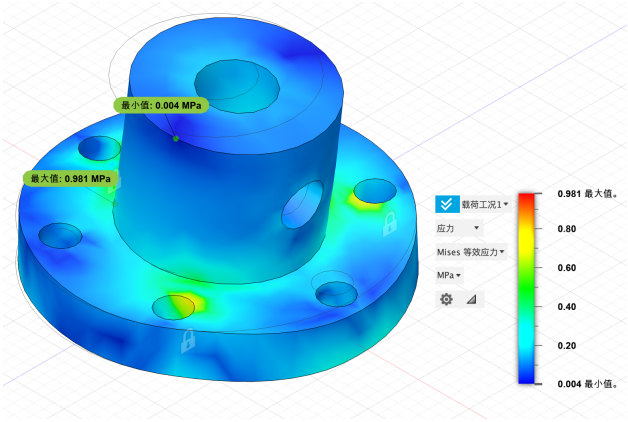

Figure 15: **Flanged Metal Connectors Stress**

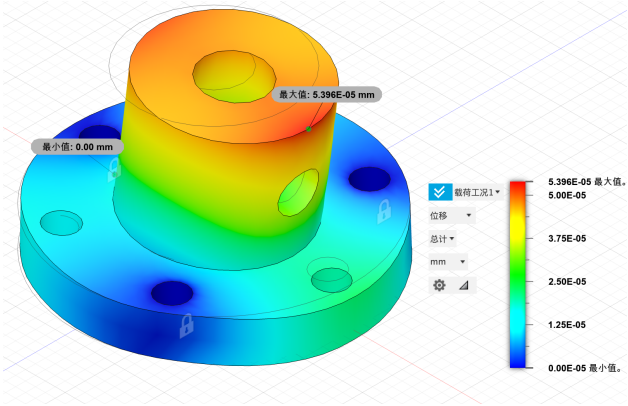

Figure 16: **Flanged Metal Connectors Displacement**

4 Cost

4.1 Labor

The labor cost for our project is as follows (Tab. 4.1): We have selected the average salary of UIUC graduates as our hourly wage, which amounts to $35 per hour. Subsequently, we estimate the total working hours required to complete the project based on our workload and course credits. Assuming a reasonable salary, the calculation is as follows: ($35/hour) x 2.5 x hours to complete = TOTAL.

Member	$/Hrs	Hrs/Week	Weeks	Multiplier	Total
ZIYUE GUO	35	20	14	2.5	$24,500
ZONGYANG ZHU	35	20	14	2.5	$24,500
YIZHI LI	35	20	14	2.5	$24,500
YIQUAN JIN	35	20	14	2.5	$24,500
TOTAL	140	20	14	2.5	$98,000

Table 4: **Labor Cost Analysis**

4.2 Parts

The following (Tab. 4.2) is a table listing all hardware parts (description, manufacturer, part #, quantity, and cost). We estimate the hardware cost to be ¥ 3958, which is approximately $548.

Name	Description	Manufacturer	Part #	Quantity	Cost	Total
Battery	12V 5000mAh DC Lithium Battery	WHEELTECH	E353S	1	¥ 119	¥ 119
Wireless Charging Coils	100W24V4A high-power and high-efficiency wireless charging Coils	WP	WP3640T WP2450R	1	¥ 120	¥ 120
Motor	12V DC Metal Gear Reduction Motor	WHEELTECH	MG513P30	4	¥ 79	¥ 316
Camera	ASTRA S RGBD Camera	ORBBEC	ASTRA S RGBD	1	¥ 960	¥ 960
Radar Sensor	Time-of-Flight (TOF) LiDAR sensor	LEISHEN	N10P	1	¥ 479	¥ 479
Micro-controller STM32	C30D ROS Four Wheel Drive MCU	ST-Microelectronics	STM32-F407VET6	1	¥ 379	¥ 379
Rasberry Pi 4B	Rasberry Pi 4B (CPU GPU/NPU 64G MicroSD)	Rasberry Pi	Rasberry Pi 4B	1	¥ 778	¥ 778
Chassis	R3 Series Four-wheel Drive Chassis	WHELLTEC	R3S	1	¥ 759	¥ 759
Shock Absorber	Oil Pressure Shock Absorber 75mm	Riaario	AM-X12	2	¥ 24	¥ 48
Total						¥ 3958

Table 5: **Hardware Cost Analysis**

5 Conclusion

5.1 Accomplishment

Overall, we have had some more meaningful achievements in this program. First, we designed a chassis system that allows the cart to move well on uneven ground. Secondly, we realized the radar obstacle avoidance function, so that the car can judge whether it can pass through the corresponding passage to avoid collision with obstacles. We also implement a depth camera that recognizes the corresponding color blocks and prompts the cart to stick to the blocks, thus helping the cart to recognize the charging station. Finally, we have implemented a series of circuit designs on the PCB board to realize the wireless charging and power monitoring functions of the cart.

5.2 Uncertainties

For the uncertainties in the project, we believe that there is some uncertainty in the accuracy of the cart's parking position in recognizing the color blocks and thus automatically finding the charging post, which may be affected by the terrain and the quality of the ambient light on the color recognition function. Another uncertainty is the volatility of the wireless charging power, which can be affected by environmental factors thus causing power instability.

5.3 Ethical and Safety

5.3.1 Ethical Issues

Ethical Issues of High-Power Wireless Charging Autonomous Vehicles:

1. **Privacy Concerns:** The wireless charging system may require communication with the vehicle to better manage the charging process. This communication may involve information such as the vehicle's location and driving habits. Ensuring the privacy of this data, preventing misuse, and unauthorized access raises ethical considerations regarding user privacy [2]. We promise that our project will adopt security measures according to law so as to not invade user's privacy by following the ACM Code of Ethics, 1.6, "taking precautions to prevent re-identification of anonymized data or unauthorized data collection, ensuring the accuracy of data, understanding the provenance of the data, and protecting it from unauthorized access and accidental disclosure." [3]
2. **Social Equity:** The widespread adoption of high-power wireless charging technology may face issues of social equity. If the implementation of this technology is predominantly limited to specific regions or socioeconomic groups, it could exacerbate technological divides, leading to ethical concerns related to social fairness.
3. **Emergency Handling:** In emergency situations such as fires or accidents, the ethical responsibility for safely interrupting the charging process and ensuring the safety of the vehicle and the surrounding environment comes into play.

5.3.2 Safety Issues

Safety Issues of High-Power Wireless Charging Autonomous Vehicles:

1. **Electromagnetic Radiation:** High-power wireless charging systems may generate strong electromagnetic radiation, posing safety risks to individuals, animals, and other electronic devices. Ensuring that the system complies with relevant electromagnetic radiation safety standards is critical to reducing potential health risks.
2. **Charging Speed and Battery Life:** Pursuing excessively fast charging speeds may negatively impact battery life and performance. Safety-wise, it is necessary to balance charging speed and battery health to ensure the safe operation of the vehicle and preserve battery life.
3. **System Failures and Safety Standards:** The design and implementation of high-power charging systems must adhere to strict safety standards [4]. System failures could lead to fires or other safety issues, necessitating measures to ensure the system can operate safely in various conditions, including emergency shutdown and fault-handling mechanisms.
4. **Energy Source and Environmental Safety:** If the charging system primarily relies on non-renewable energy sources, it could have adverse environmental impacts. Ensuring the use of clean, renewable energy sources is a crucial safety issue to reduce the risks of environmental pollution and climate change [5].

References

[1] Z. Huang, S.-C. Wong, and K. T. Chi, "Design of a single-stage inductive-power-transfer converter for efficient ev battery charging," *IEEE Transactions on Vehicular Technology*, vol. 66, no. 7, pp. 5808–5821, 2016.

[2] J. Robinson, J. Smyth, R. Woodman, and V. Donzella, "Ethical considerations and moral implications of autonomous vehicles and unavoidable collisions," *TheoreTical issues in ergonomics science*, vol. 23, no. 4, pp. 435–452, 2022.

[3] D. Gotterbarn, B. Brinkman, C. Flick, *et al.*, "Acm code of ethics and professional conduct," 2018.

[4] R. L. B. Pinkus, *Engineering ethics: Balancing cost, schedule, and risk-lessons learned from the space shuttle*. Cambridge University Press, 1997.

[5] T. Muneer, M. Kolhe, and A. Doyle, "Electric vehicles: Prospects and challenges," 2017.

A Appendix A: Related Figures

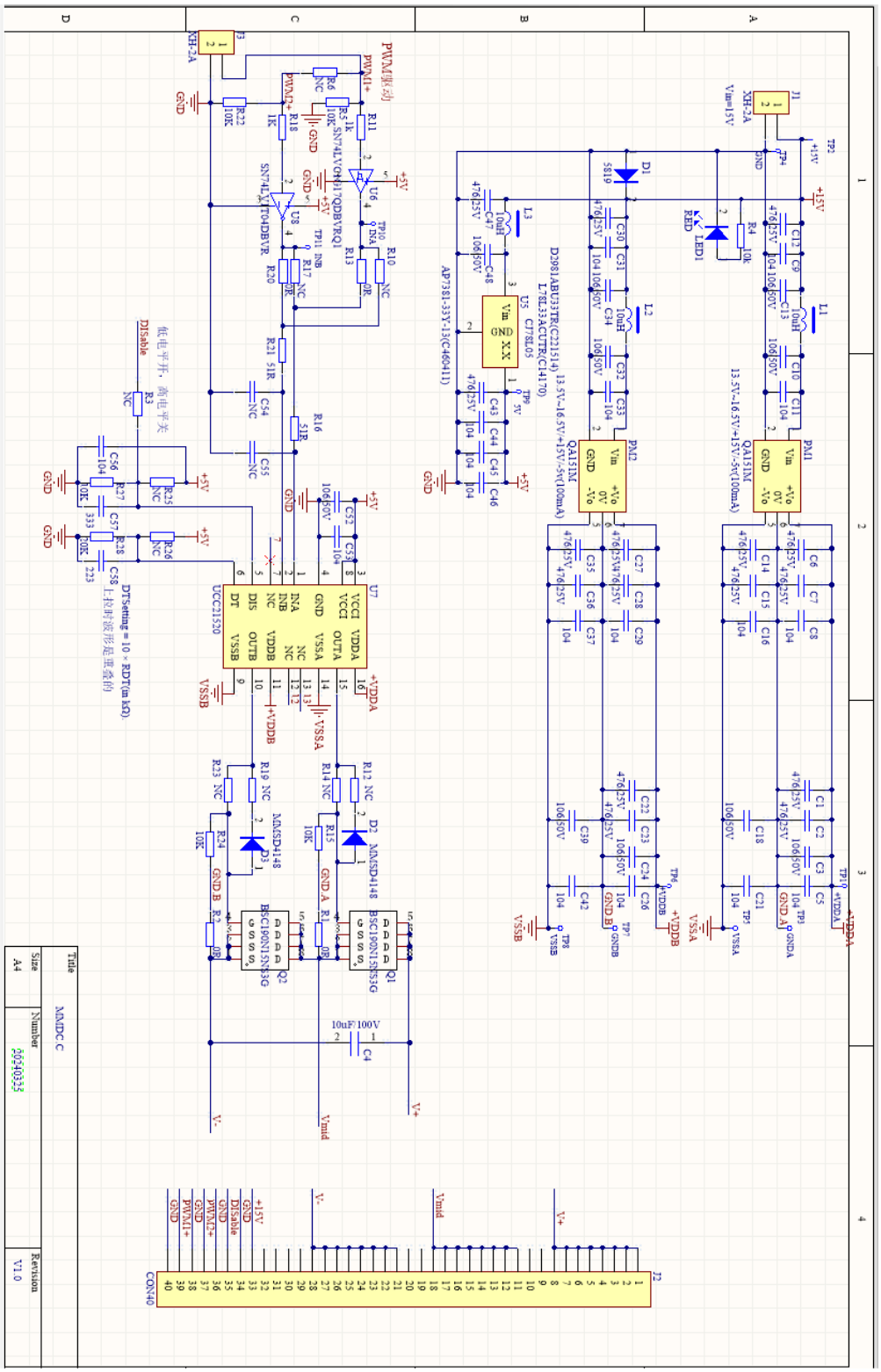

Figure 17: **Schematic PCB Design of Inverter and MOSFET Driver Circuit**

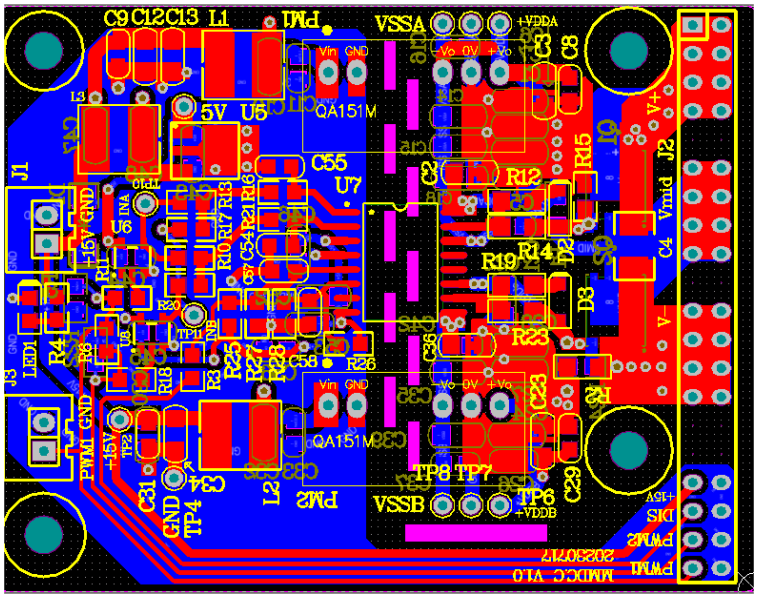

Figure 18: **Layout PCB Design of Inverter and MOSFET Driver Circuit**

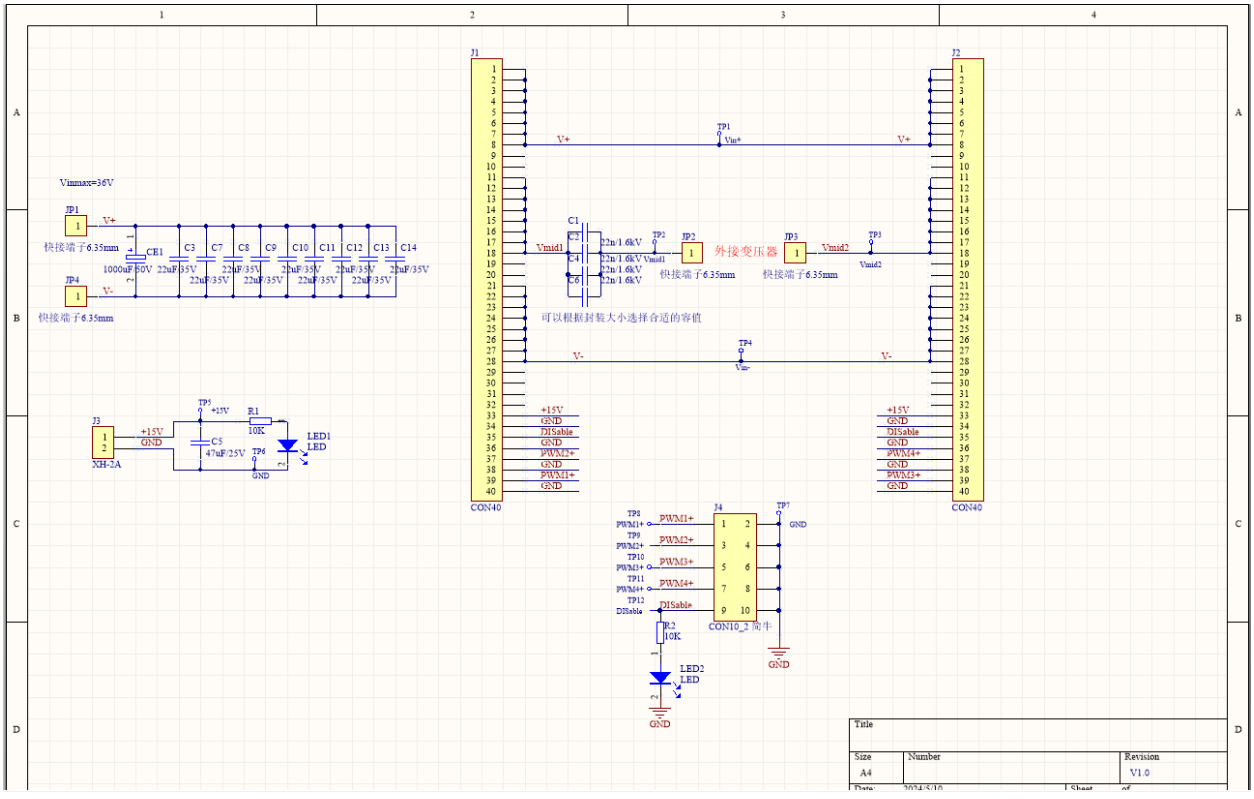

Figure 19: **Schematic PCB Design of the Resonant Circuit on the Transmitter Side**

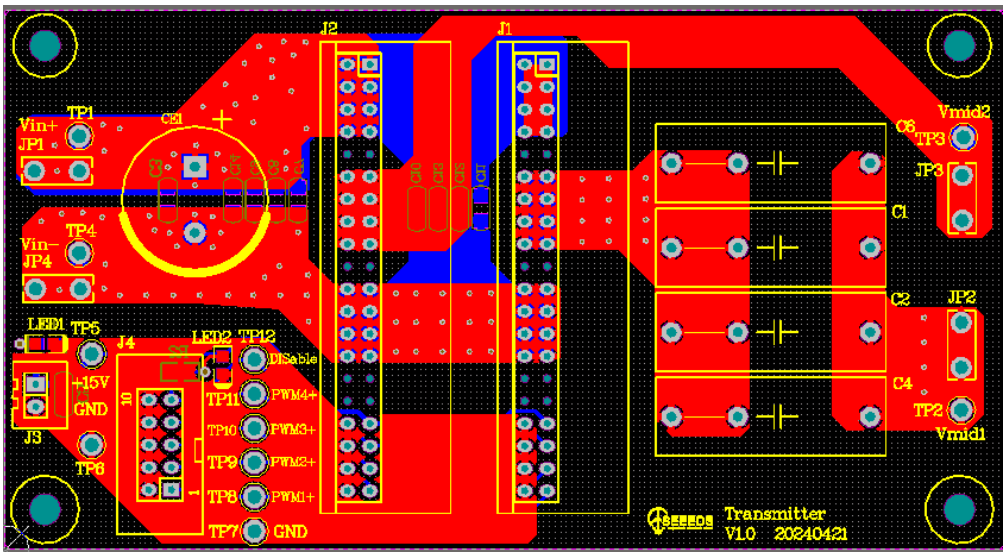

Figure 20: **Layout PCB Design of the Resonant Circuit on the Transmitter Side**

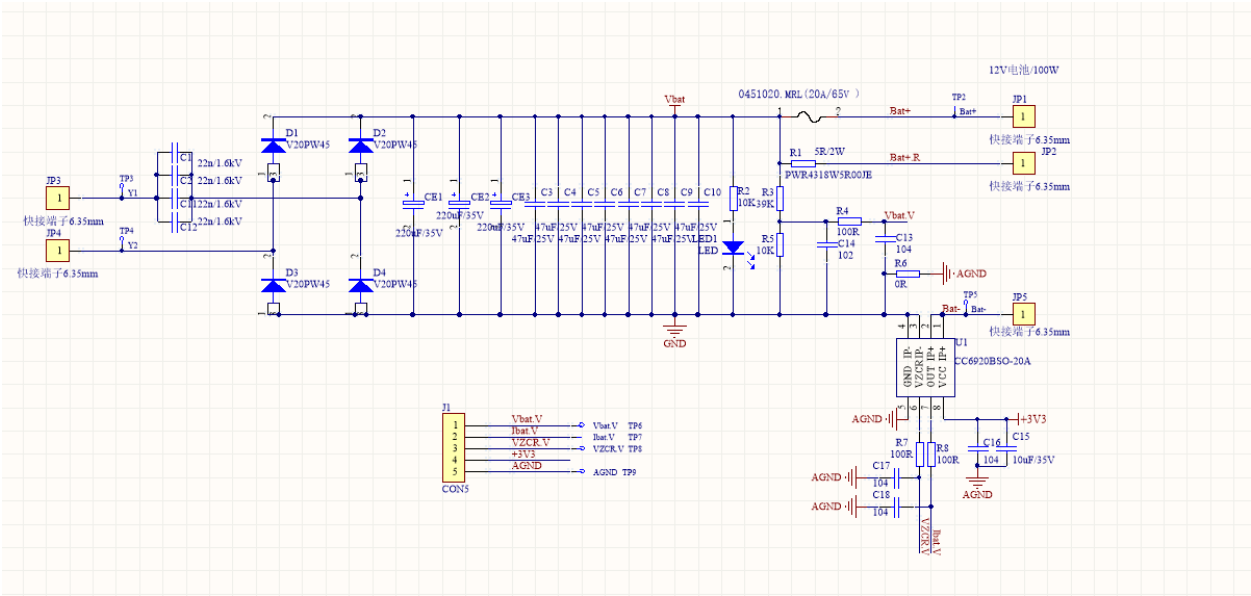

Figure 21: **Schematic PCB Design of the Circuit on the Receiver Side**

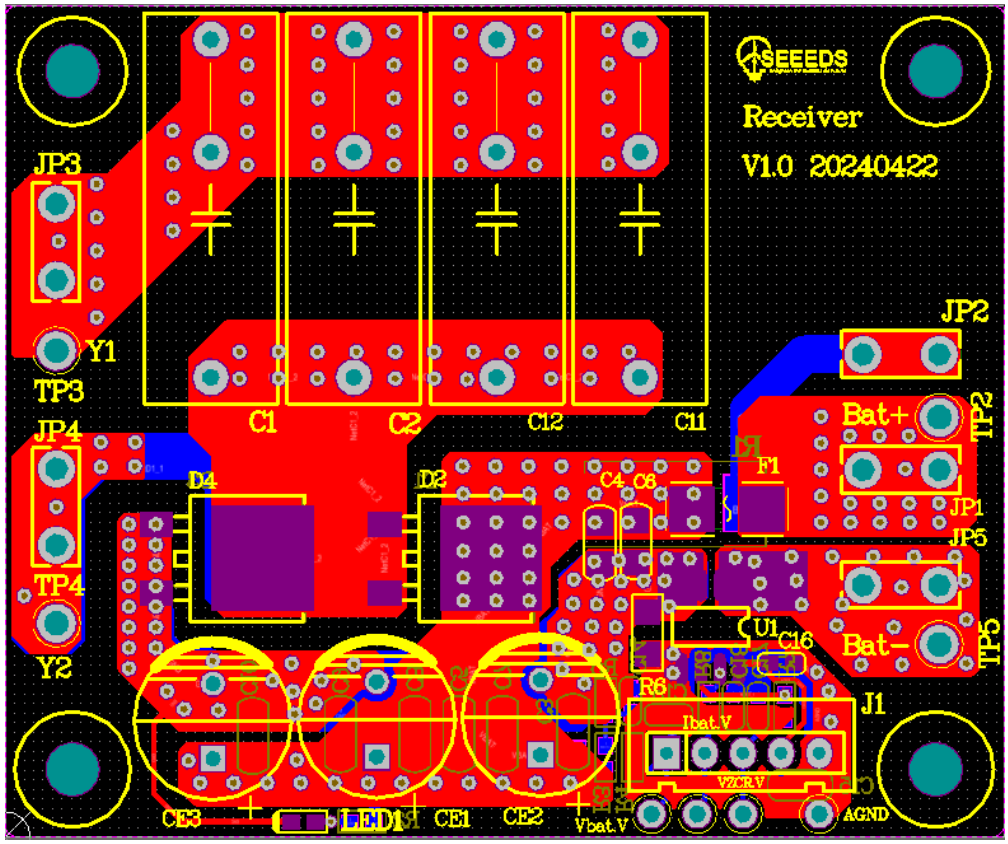

Figure 22: **Layout PCB Design of the Circuit on the Receiver Side**

B Appendix B: Points Summary

Task	Requirements	Points
Wireless Charging	Battery charging power $>$ 12W	5
	The display screen has the charging power	4
	Buzzer alarm upon completion of charging	3
	PCB can sample the battery voltage	3
Remote Contorl Car Motion & Mapping	Computer-controlled car omnidirectional movement	10
	Utilize LiDAR to detect obstacles and construct maps	10
Sensor Functionality	Ability to freely move to specified locations in the map	5
	Utilize RGB camera for object recognition and tracking	5
Mechanical Structure	Chassis shock absorption structure	5
Total	\	50

C Appendix C: Requirement and Verification Table

C.1 Drive Subsystem

Requirements	Verification
1) Use four PWM drives to independently adjust the speed and direction of the four motors.	1) Use oscilloscope to check the current passing the motor. When the current is positive, the motor rotates clockwise.
2) The rated power of the designed motor is 4.32W and the rated torque is 1kg*cm	2) Test the speed and kinetic energy of the car to calculate the actual power.
3) The car is capable of omnidirectional movement.	3) Issue movement commands to the car using a computer and observe its behavior.

C.2 Wireless Charging Subsystem

Requirements	Verification
1) Once aligned with the charging point, the car implements fast wireless charging with over 12W power.	1) An oscilloscope and a multimeter were used to sample various parameters in the primary and secondary circuits, and the charging power was calculated.
2) The circuit can sample the battery voltage and charging current, and the power meter can display the charging power during charging.	2)The circuit can sample the battery voltage and charging current, and the power meter can display the charging power during charging.
3)The buzzer will alarm upon the completion of charging.	3)Monitor whether the battery voltage exceeding the threshold voltage will trigger an alarm.

C.3 Sensor Subsystem

Requirements	Verification
1) Ensure that the power supply interface is correct and the current is safe and stable.	1) Data transmission is facilitated via USB 2.0 connectivity. Other parameters also need to be matched with each sensor.
2) Ensure that the camera can identify surrounding environments in real-time, discerning patterns such as zebra crossings and traffic lights.	2) We will initially conduct photo tests using the camera to evaluate whether its resolution, field of view (FOV), and other parameters meet requirements. The captured images will then be uploaded to an image recognition algorithm to assess its accuracy in detection.
3) Ensure the radar can detect surrounding obstacles and transmit signals to the processor	3) Use an oscilloscope to test whether the radar output signal is normal.

C.4 Processor Subsystem

Requirements	Verification
1) Isolates electromagnetic waves during wireless charging to protect circuit components and ensure normal circuit operation.	1) A: Install magnetically shielded components and place the cart as a whole in a 100W electromagnetic wave environment. B: Observe the operation of the circuit and controller to ensure that the circuit operates normally.

C.5 Chassis Subsystem

Requirements	**Verification**
1) Maintaining the relative level of the cart chassis on uneven ground improves wireless charging efficiency.	1) A: The cart-mounted shock absorbing structure was placed on a test surface with level ground on the left and a ten-degree slope on the right. B: Calculate the wireless charging efficiency, which is above eighty-five percent.
2) Maintaining the stability of the overall attitude of the cart ensures the efficiency and accuracy of the depth camera recognition.	2) A: The cart-mounted shock absorbing structure was placed on a test surface with level ground on the left and a ten-degree slope on the right. B: Observe the camera recognition, the camera recognizes the roadway and signs ahead normally.